Results from the APPU project
The potential of low-threshold hydrogen-powered BLI propulsion

Heidebrecht, Alexander; Hoogreef, Maurice; Isikveren, Askin T.; Rao, Arvind Gangoli

Publication date
2024

Document Version
Final published version

Published in
34th Congress of the International Council of the Aeronautical Sciences, ICAS 2024

RESULTS FROM THE APPU PROJECT: THE POTENTIAL OF LOW-THRESHOLD HYDROGEN-POWERED BLI PROPULSION

Alexander Heidebrecht[1], Maurice Hoogreef[1], Askin T. Isikveren[2] & Arvind Gangoli Rao[1]

[1]TU Delft, Netherlands
[2]SAFRAN S.A. c/o Aerospace Embedded Solutions GmbH, 80639 Munich, Germany

Abstract

Results from the APPU project, which investigated the concept of an "Auxiliary Power and Propulsion Unit" (APPU) are presented. The APPU is a hydrogen-driven boundary-layer-ingesting engine at the tail end of a passenger aircraft which replaces the conventional APU and contributes about 15% of total thrust at top of climb. The aim of the configuration is to allow the introduction of hydrogen and BLI technology by upgrading existing aircraft designs. The concept aims to benefit from the advantages of these new technologies as much possible, without requiring the same level of reliability as for conventional propulsion, during times when hydrogen infrastructure is not universally available. The investigation concerns hydrogen tank mass, engine efficiency, operational, aerodynamic and reliability aspects, and finds block CO_2 emissions can be reduced by a larger amount than the thrust rating of the auxiliary hydrogen engine may suggest. One reason for this is that the additional engine permits smaller and more efficient designs for the main engines. A still larger benefit is found to arise out of the assumption that the APPU engine and associated H_2 fuel systems is less reliable than the conventional underwing engines. This assumption permits different strategies to maximize the utilisation of hydrogen over kerosene. CO_2 emissions for the design mission are found to be reduced by 23.1% over the A321neo, and by 15.5% over an A321neo fitted with updated turbofan engines.

Keywords: keywords list (Boundary Layer Ingestion, hydrogen aircraft, conceptual aircraft design)

Nomenclature

Abbreviations

APPU	Auxiliary Power and Propulsion Unit
APU	Auxiliary Power Unit
BLI	Boundary Layer Ingestion
CFD	Computational Fluid Dynamics
IPF	Installed Propulsive Force
LCI	Layered Composite Insulation
LTO	Landing and Take-Off
MLI	Multilayer Insulation
OEI	One Engine Inoperative
ToC	Top of Climb

Symbols

c_P	pressure coefficient (–)
E	energy (J)
H	altitude (m)
M	Mach number (–)
m	mass (kg)
NVF	Net Vehicle Force (N)
P	Power (Wg)
$tsfc$	thrust-specific fuel consumption $(\frac{g}{s \cdot kN})$
$tsfc'$	equivalent $tsfc$ $(\frac{g}{s \cdot kN})$
$tsec$	thrust-specific energy consumption $(\frac{W}{N})$
α	aircraft angle of attack $(^\circ)$
Δm	mass difference: $m - m_{ref}$
$\mathbf{Q}E$	rel. change in Energy: E/E_{ref}
$\mathbf{Q}m$	rel. change in mass: m/m_{ref}
η	efficiency (–)
Φ_{inst}	installed propulsive force (N)

Suffixes

act	actuator disk
$appu$	APPU engine and propulsor
$cone$	fuselage tailcone
$core$	(APPU) engine core
cr	cruise

eng	engine	ref	reference case
k	kerosene	TO	Take-off
blk	block (design mission w/o diversion)	tot	sum of all components
$prop$	propulsor	ToC	Top of Climb

1. Introduction

The APPU (Auxiliary Power and Propulsion Unit) concept replaces the APU (Auxiliary Power Unit) in the tailcone of a conventional passenger plane with an auxiliary engine which is capable of running on hydrogen. The study shown here uses an Airbus A321neo as the baseline. In addition to enabling use of a new fuel, the engine also makes use of Boundary-Layer Ingestion (BLI)[1], which promises a notable reduction of mechanical power required for a given amount of thrust, and has been the object of several studies on future transport aircraft [2, 3, 4]. Implementing these new technologies in an auxiliary engine which is significantly smaller than the conventional engines is intended to allow much faster introduction to the market, since it can be implemented by modifying existing designs rather than requiring entirely new aircraft. It is also expected to reduce the technological – and therefore the economical and operational – risk of introducing radically new technology, since lack of hydrogen fuel or non-critical malfunctions of the new systems leave the conventional part of the propulsion system unaffected. A previous investigation of the concept has found a large degree of commonality [5], as can be seen in figure 1. The forward part of the aircraft stays unchanged, save for the insertion of two fuselage frames forward of the wing and the removal of two frames aft of the wing, needed to align the wing position to the centre of gravity after modifying the tailcone and installing additional components. Figure 2 shows details of the original and modified geometry of the aircraft tail. The fuselage of the modified aircraft is longer than the original by 77cm, and the empennage is reconfigured to a T-tail or cruciform, in order to avoid interaction of the BLI propulsor with the wake of the horizontal tailplane and create the necessary space for the LH_2 tank.

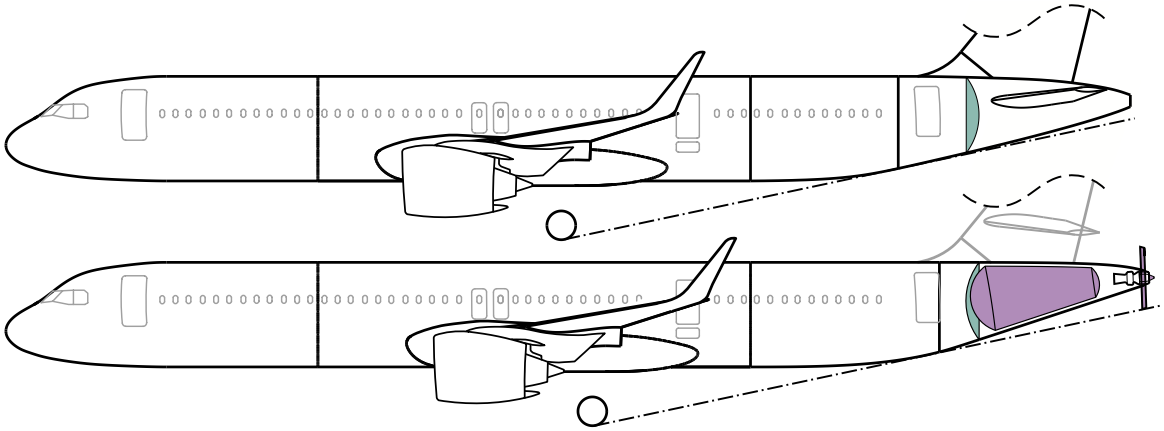

Figure 1 – Side view of the baseline A321neo (top) and the modified "APPU" version with shifted wing, remodelled tailcone and open rotor (bottom)

Following earlier investigations [5, 6] focussed on mass estimates and conceptual aircraft design methods, this paper presents further, higher-fidelity analysis, different sizing strategies, and investigates the resulting impact on the configuration.

The LH_2 tank mass estimate is updated compared to earlier publications [5], and an upgrade of the main engines is considered. The study investigates the degree to which the main engines can be lighter and more efficient when taking the thrust contribution from the new APPU engine into account in the sizing process, and how this affects block fuel burn. To this end, parametric engine models are used which provide an estimate of how the engines, their mass and fuel consumption may change depending on thrust requirements.

In an effort to investigate certification of an APPU unit, the impact of assuming different levels of reliability of the APPU engine and H_2 fuel systems is regarded, in conjunction with operational strategies for distributing the required thrust between the main engines and the APPU engine.

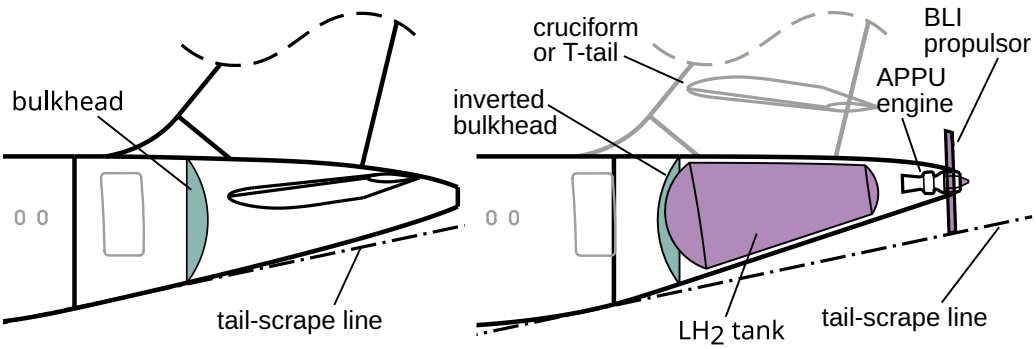

Figure 2 – Close-up of the tailcone geometries of the A321neo (left) and the modified version with a LH_2 tank of 14.6m^3 gross volume(right)

The analysis is supported by CFD simulations of the original and modified fuselage tailcone, in order to obtain more accurate estimates of additional drag, the propulsive benefit and power requirement caused by the BLI propulsor. Its effect on the flow was simulated using an actuator disk, which in combination with an engine cycle model provides a means to determine the effective thrust contribution of the APPU engine, its fuel consumption, and in combination with the overall aircraft analysis, its impact on kerosene burn and CO_2 emissions.
The fuel consumption of the resulting design is compared to the baseline A321neo aircraft as well as to a hypothetical varient with upgraded turbofan engines. Section 2. lays out the methodology for the various sizing, performance and analysis methods. The approach used to investigate the impact of reliability was developed for this study and is shown in section 2.6. In the Results section, the different inputs are linked, and effect of the APPU engine on block kerosene is characterized. This is done first while assuming perfect reliability, and section 3.5 shows the impact of assuming non-perfect reliability on mission fuel energy and kerosene burn.

2. Methods

2.1 Fuel burn analysis

The study uses a simplified mission fuel burn analysis, linking multiple component performance models and/or sizing methods. It was decided not to include analysis of climb and descent phases since no sufficiently-consistent model of the BLI propulsor efficiency was available to generate credible maps of $tsfc$ and thrust capability for the APPU engine. Therefore, the impact on those flight phases on mission fuel burn and e.g. climb performance was not regarded. The analysis focussed on the maximum-range mission with maximum payload of the "WV053" weight variant[8], which has a range of 4630km, a payload of 25t, and cruises at 10058.4m altitude (33kft) with a Mach number of 0.78.
Since the analysis uses constant altitude and Mach number, it was necessary to adjust engine $tsfc$ values to mission-averaged values, such that the fuel-burn analysis of the reference aircraft matched the previously-determined block fuel. For this purpose, the block fuel and reserve fuel amounts were determined by splitting the known total fuel mass at take-off [8], using the ratio of block fuel to reserve fuel found by reproducing the design in *Initiator*[7]. The engine $tsfc$ values were adjusted by a factor determind such that the fuel burn analysis of the reference aircraft matched the previously-determined block fuel. The diversion phase was then modelled as continuing the flight for the appropriate distance over which the reference aircraft burns all reserve fuel. The $tsfc$ correction factor and diversion distance found for the reference aircraft were applied to all configurations in this study. More detail can be found in a previous publication [5].
The fuel burn analysis of different variants of the APPU aircraft permits specifying either constant throttle or constant thrust share between the main engines and APPU engine, with the limitation that throttle may never exceed 100%, as well as the fuel type used by the APPU engine. These inputs can be set differently for different phases of the mission (i.e. the diversion phase may use different settings). The tool also includes routines to iteratively adjust either the APPU thrust share or the LH_2 tank size such that all usable LH_2 fuel is consumed by the end of the mission, and likewise adjust kerosene mass at take-off.

The analysis method is linked to sizing methods for the hydrogen tank, APPU engine and main engines, acording to given thrust/weight ratios for OEI operations at take off and at the start of the diversion, as well as minimum climb requirement at Top of Climb (ToC). The OEI sizing was based on the known ratio of take-off mass to maximum take-off thrust of the reference aircraft and its engines[9], with incremented thrust required in scenarios when the aircraft was assumed to have three operative engines.

2.2 Tank mass and size

A parametric model for the hydrogen tank was established using a modified version of the model by Onorato [10], assuming a double-walled tank, and vacuum-assisted insulation. The tank mass model accounts for structural mass of the pressure vessels including stiffeners and structural connection to the fuselage, as well as residual H_2 and hydrogen fuel systems.
Based on previous studies, the largest feasible LH_2 tank size was selected, assuming a minimum wall distance of 0.15m between the outer mould-lines and the inner volume. This assumes 50mm thickness for both pressure shells and insulation, which is conservative compared to findings from the CHEETA project [11] that a double-walled tank of 24mm total wall thickness, including stiffeners, is possible, of which only 16mm are occupied by insulation. This is mainly based on the use of vacuum multilayer insulation (MLI) or composite layers of MLI with other types of novel insulation material (Layered Composite Insulation, LCI). Such materials can achieve thermal conductivity more than two orders of magnitude below that of conventional foams [12] thus 20mm of LCI insulation could theoretically replace conventional foam of 2m thickness. While this impressive, it is assumed that early implementations may not be able to take full advantage of this capability, and require measures which reduce the insulation effectiveness or increase its thickness. These measures could consist of additional dividers or spacers, or of redundant layers with acceptable insulation properties in atmospheric pressure, e.g. aerogel blankets, to limit the heat influx to manageable levels if vacuum should be lost. By reserving more than twice the space for insulation as found by the CHEETA project, it should also be possible to meet any reasonable requirement for dormancy time. An additional 100mm are taken up by frames which stiffen the external shell, on the outside of the tank, as proposed by Montellano [13]. While Montellano shows that it is feasible to construct a structurally-integral tank in this way, the current study neglects any savings in structural mass of the tailcone, in favour of a pessimistic mass estimate.

2.3 Turbofan engines

The cycle of the underwing engines was modelled engine engine cycle analysis for two-shaft turbofans based on handbook methods[14]. It was extended to permit producing full-factorial maps of engine $tsfc$ as a function of altitude, flight Mach number and throttle setting, and to allow constrained optimisation of engine cycles. To this end, the engines of the reference A321neo were first modelled by replicating known engine data [9, 15].
Constrained optimisations were conducted to obtain a number of plausible next-generation turbofan engine cycles for a range of thrust requirements. For these next-generation engines, it was assumed that overall pressure ratio was limited to 55, bypass ratios could increase up to 16, turbine entry temperature above 1800K could not be sustained, and fan radius could increase by 10% over the current engines.
Since the fuel burn analysis uses a mission-averaged $tsfc$ for the reference engines (see section 2.1), the resulting design $tsfc$ values were adjusted by the ratio between the mission-averaged $tsfc$ and the value found for the reference engine at design conditions.
Similarly, the resulting mass estimates for the turbofan engines were scaled with the ratio between the mass estimate for the reference engine and the known dry engine mass [9]. To investigate the effect of an engine upgrade on the APPU configuration, the engine mass and $tsfc$ were then interpolated from the series, dependent on the thrust requirement of the respective configuration. This leads to a variable main engine mass and $tsfc$, as a function of the APPU engine contribution and whole-aircraft thrust requirement. The correlation used for this study is shown in figure 3, compared to the current engines. Table 4 shows the values of installed mass and $tsfc$ for the reference engine, two variants of the next-generation turbofan engines and the APPU engine.

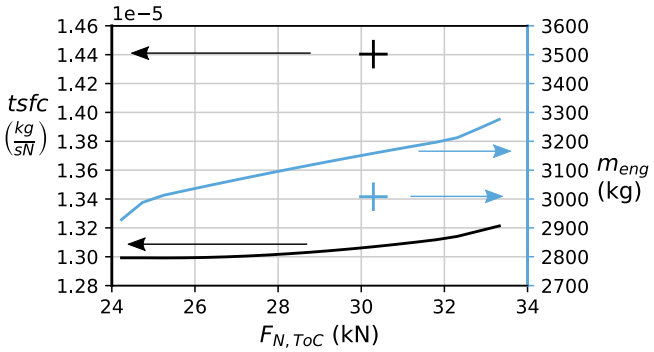

Figure 3 – Thrust-specific fuel consumption (black) and dry engine mass (blue). Crosses indicate estimate for the CFM LEAP-1A engine, curves show the projection for the future engine design, as a function of the design thrust at Top of Climb (ToC).

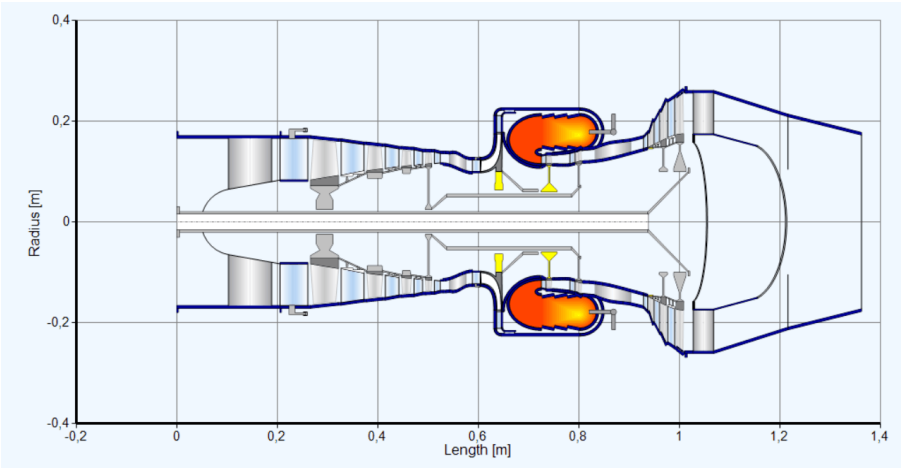

Figure 4 – Engine geometry generated by GasTurb, based on engine cycle optimized in PyCycle. Note that GasTurb always extends the power shaft to the front of the engine, but this is not necessarily required for the APPU engine. Figure by Martin van Schie[17]

2.4 APPU engine core

The APPU engine core is projected to be a 2-shaft turbo core with a separate power turbine, driving a single open rotor which is located downstream. Although this requires placing the rotor gearbox close to the hot exhaust stream, it permits an annular exhaust, thus avoiding issues with base flow on a rotating backwards-facing spinner and allowing the exhaust to contribute to overall thrust. Placing the rotor as far aft as possible also reduces the impact it has on empennage design, since no critical part of the empennage may be located within our downstream of the rotor plane. The engine has a conventional axial low-pressure compressor and a radial high-pressure compressor. This allows it to achieve an overall compression ratio of 25 or higher, despite a comparatively low core mass-flow. This design also permits a reversed combustor chamber, which in turn permits the engine to be shorter than possible with a conventional arrangement.

The design shaft power at cruise altitude was estimated based on the maximum feasible LH_2 tank size and the estimated engine core efficiency, such that the APPU engine can make use of all usable hydrogen during the reference mission. This resulted in a design shaft power of 2.2MW in total, of which 2MW are supplied to the rotor and the remaining 0.2MW used for on-board power.

The engine cycle was initially modelled in GasTurb [16], and further improvement was part of a separate study [17], using PyCycle. This took into account that the APPU engine core ingests air from the near-wall region of the tailcone boundary layer, and that static pressure at the core exhaust is increased above ambient conditions. Figure 4 shows the projected shape and size of the engine, as constructed by GasTurb, using the component sizing obtained during the cycle optimisation.

While the above engine design study also investigated further efficiency gains by using the cold H_2

drawn from the LH_2 tank as a heat sink, for water recovery from the exhaust, such potential benefits were ignored in the study presented here. The predicted thermal efficiency is 44.5%. For the purpose of this study, a lower value of η_{core}=0.43 was used to represent the rate at which the energy stored in the fuel is converted to shaft power. This was done to account for additional cooling required for the downstream gearbox and other potential sources of losses.

2.5 BLI propulsor, Thrust & Drag Accounting

There is currently no accepted analytical method to calculate the "thrust" and "efficiency" of BLI engines. The relationship of power applied to the flow and propulsive force produced was obtained using CFD simulations of a "clean" fuselage tailcone. These represented the geometry of the fuselage with the reference tailcone geometry and vertical tailplane (vtp), but omitted the wing since wing downwash is expected to have only a minor impact on the design, as well as the horizontal tailplane (htp), since it is likewise not influencing the flow field around the propulsor in the APPU configuration. While this removes the ability to estimate the absolute drag of the aircraft, it also removes the necessity to create a realistic and well-designed wing/body junction as well as empennage design for the reference and modified aircraft, and to ensure correct trim of the htp in order to achieve a realistic drag value and downstream wake.

A first estimate was based only on the flow about the reference geometry in combination with isentropic 1D theory. The net momentum added to the flow by the propulsor was estimated by assuming that the propulsor provides isentropic compression with a constant total pressure ratio across the disk, and isentropic expansion from the disk to far-field static pressure. This provides an estimate of the propulsor power required after viscous and compressibility losses on the rotor and power lost to swirl, and finds a 30% lower power requirement for a BLI rotor of 4.5m^2 rotor area, compared to a turbofan engine modelled similarly, by incrementing total pressure in an accordingly smaller free-stream streamtube. This estimate is however very optimistic and has to be regarded as an upper bound in ideal flow, since e.g. the efficiency of an open BLI rotor in transonic flow is unlikely to match that of a ducted fan, and it disregards the interaction between the rotor and the forces on the fuselage tailcone.

A more "holistic" estimate was obtained by conducting further CFD simulations which also simulated the flow around the modified tailcone, with and without active propulsor, at varying powers. Since the flow cannot be cleanly split into thrust and drag domains according to AGARD recommendations for thrust and drag accounting [18], all comparisons took place on the level of the Net Vehicle Force (NVF), which represents the integral of all aerodynamic forces on the aircraft. A separate study concerned itself with the design of a submerged intake and exhaust for the engine core [19], but did not model the propulsor.

By comparing the different simulation outcomes, the difference between the forces on the reference tailcone and the fully modified tail with installed engine and propulsor can be split into various components. ΔNVF_{cone} (equation 1) is the effect of modifying the tailcone without applying power to the flow, ΔNVF_{core} (equation 2) the effect of installing and operating the engine core with intake and exhaust, operating at design power, and ΔNVF_{prop} (equation 3) represents the influence of the propulsor, as function of the applied power. In combination, they represent the total effect of the modifications on the streamwise force balance.

$$\Delta NVF_{cone} \coloneqq NVF_{mod,P_{act}=0} - NVF_{ref} \tag{1}$$

$$\Delta NVF_{core,cr} \coloneqq NVF_{core,cr} - NVF_{mod,P_{act}=0} \tag{2}$$

$$\Delta NVF_{prop}(P_{act}) \coloneqq NVF_{mod}(P_{act}) - NVF_{mod,P_{act}=0} \tag{3}$$

Since the simulations with actuator disk were conducted with varying power applied to the actuator disk, the results can be interpolated to a different actuator power. For the engine core and the efficiency of the propulsor itself, only data at the design condition is known, therefore the effect of the core on NVF is assumed to be linearly dependent on the output power. With this, the net effect of modifying the tail, installing and operating the BLI propulsor on the streamwise force balance can be

computed, in the form of the installed propulsive force (Φ_{inst}), shown in equation 4.

$$\Phi_{inst,APPU}(P_{act}) = \Delta NVF_{cone} + \Delta NVF_{core,cr}\frac{P_{act}}{P_{act,cr}} + \Delta NVF_{prop}(P_{act}) \tag{4}$$

Since thrust is not cleanly defined for BLI applications, but the fuel burn analysis requires a value for $tsfc$, the thrust/drag split is based on the components of $\Phi_{inst,APPU}$: ΔNVF_{cone} is regarded as additional airframe drag since it is independent of APPU engine power output. The two other terms in equation 4 depend on engine power and are accounted for as effective thrust. If the fuel flow in a given condition is known, this results in an *equivalent* specific fuel consumption ($tsfc$') of:

$$tsfc'_{APPU} = \frac{\dot{m}_f(P_{act})}{\Delta NVF_{core,cr}\frac{P_{act}}{P_{act,cr}} + \Delta NVF_{prop}(P_{act})} \tag{5}$$

Note that while equation 5 permits the calculation of fuel flow in the same way as $tsfc$ for conventional engines, it is not based on the same definition of thrust, which for example means that it can *not* be used to calculate a physically meaningful value of propulsive efficiency, η_P. The efficiency of the propulsor itself in applying shaft power to the flow can be expressed as $\eta_{prop} = P_{act}/P_{shaft}$, that is the amount of power needed by a perfect actuator disk to achieve a certain ΔNVF_{prop}, compared to the shaft power required by the propulsor in order to achieve the same effect, in the same flow field. With a given fuel energy content (LHV, Lower Heating Value) and engine core efficiency, this permits estimating the fuel flow (equation 6).

$$\dot{m}_f(P_{act}) = \frac{P_{act}}{LHV_f \cdot \eta_{core} \cdot \eta_{prop}} \tag{6}$$

Since an estimate of propulsor efficiency could only be obtained for the cruise condition, limiting fuel burn analysis to flight at cruise altitude, and since $\Delta NVF_{prop}(P_{act}$ was found to be nearly a linear function, $tsfc$' was assumed to be approximately constant for the investigated range, and equal to the specific fuel consumption in cruise, shown in equation 7.

$$tsfc'_{APPU,cr} = \frac{P_{act,cr}}{LHV_f \cdot \eta_{core} \cdot \eta_{prop}\left(\Delta NVF_{core,cr} + \Delta NVF_{prop}(P_{act,cr})\right)} \tag{7}$$

This way, fuel flow can be linked to the propulsive benefit gained from the BLI propulsor, irrespective of the choice of fuel. Note that hydrogen-operated engines can have a slight efficiency advantage over kerosene engines [20], which may be compensated by adapting turbine entry temperature or accepting reduced power [21]. In light of the degree to which the calculation of the APPU engine $tsfc$' in this study depends on assumptions, this distinction was neglected.

2.6 Reliability and Availability

It is likely that achieving the same reliability and availability as modern kerosene engines and fuel systems for hydrogen propulsion poses a large threshold for market introduction, both in terms of development time and cost. Permitting somewhat lower reliability (notwithstanding strict *safety* requirements), for the APPU engine and LH_2 fuel systems could further reduce this threshold. Sizing the aircraft to be able to compensate for some component failures permits safe operations despite this, and may significantly reduce the risk to airline operations, thus reducing both safety and financial risks.

While the effect of permitting higher failure rates on development costs cannot be credibly estimated at this point, the impact on system efficiency (i.e. aircraft mass and fuel use) was investigated for several scenarios. In addition, since LH_2 infrastructure and supply are likely not going to be universally available during the transition time for which the APPU concept is designed, the fuel burn during kerosene-only operations was also regarded.

2.6.1 Investigation approach

Regulations [22] specify permitted failure rates as a function of severity of the failure, which in turn depends on the capacity to compensate for a given failure. With regards to the APPU drivetrain, low expected reliability of the LH_2 fuel system requires additional kerosene fuel reserves at take-off, and lowered expectations of APPU engine reliability need to be countered by additional thrust capability of the main engines to permit safe operations. Going beyond safety, an additional question is whether and when to also provide the capacity to continue operations to the scheduled destination after a failure, and how this impacts fuel efficiency.

The impact of permitting a certain failure scenario on the design and the fuel burn of the aircraft can be assessed by sizing the main engines and kerosene reserves for a mission during which either the LH_2 supply or the APPU engine become unavailable at some point, and adjusting the required fuel at take-off as well as the main engine thrust requirement accordingly, to ensure that OEI thrust requirements are met at take-off and at the start of the diversion leg (aborted landing before diversion), and that the required climb rate at ToC can be achieved.

For this investigation, the fuel burn estimation process was extended to allow iterative adjustment of the target (Φ_{APPU}), while limiting engine thrust to each engine's maximum thrust. This implies that Φ_{APPU} may vary throughout the flight. The sizing of the main engines used the parametric model developed in section 2.3 and ensured that the thrust requirements at ToC and at OEI conditions at take-off mass and at the start of the diversion are satisfied in each case, by requiring the thrust-to-weight ratio to at least match that of the reference aircraft in each given situation.

The reliability study assumed that the aircraft always uses the biggest possible LH_2 tank and the same size of APPU engine for all variants.

2.6.2 Failure scenarios and required provisions

Since it is not credible at the current stage to construct a matrix of potential failures, it was decided to regard a fairly generic set of scenarios classified by several variables, shown in table 1.

Which failure?	
normal	None. All components assumed to function normally
LH_2	The LH_2 fuel system is inoperative, or no LH_2 is available for refill at an airport. The APPU engine may still operate on kerosene as fuel.
APPU	The APPU engine is inoperative, with the rotor feathered. Implies that no LH_2 fuel can be used.
When?	
Diversion	The unit functions for the scheduled flight but is not relied upon in safety-critical situations. The aircraft must be able to fly the the diversion (including go-around) without using the respective unit.
Main segment	The aircraft needs to be able to fly the entire mission with the respective unit failing at or before the start of the mission. This goes beyond safety concerns and ensures operations are not affected by reliability issues (with possible exceptions for ETOPS operations), similar to the current requirements on APU units [23].

Table 1 – Variables used to parametrize component failure scenarios to investigate impact of reliability on size of main engines and kerosene reserves

Combining the different variables yields 6 different missions scenarios, shown in table 2. For each of the missions, the engines and kerosene fuel reserves were resized using the process described in 2.1, with the additions laid out in 2.6.1, but prescribing the same APPU engine and size of LH_2 tank to all variants, while adapting the thrust requirement for the main engines and the amount of kerosene required at take-off to each mission. This yielded 6 different aircraft configurations, each of

which is able fly its respective sizing mission. They differ from each other by the size and efficiency of the main engines, and by the kerosene reserves which they need to carry at take-off.

No.	mission phase main	mission phase diversion	comment
c1	normal	normal	full 3rd engine certification
c2	normal	LH_2	H_2 fuel systems not critically reliable
c3	normal	APPU	APPU engine not critically reliable (except for take-off)
c4	LH_2	LH_2	(unplanned) lack of LH_2 may never affect flight schedule
c5	LH_2	APPU	as c4, and reduced reliability of APPU
c6	APPU	APPU	Certified as APU (failure is "inconvenience")

Table 2 – Overview of the components assumed inactive during the 6 different missions used to size the main engines and kerosene fuel at take-off, according to each reliability scenario.

For segments flown without thrust contribution from the APPU engine, it was assumed that the propulsor is feathered. Given the comparatively low thrust and the low flow velocities through the APPU rotor, the resulting drag is assumed to be negligible compared to total aircraft drag.
One notable consequence of sizing scenarios which use no LH_2 during the diversion is that all usable LH_2 may be used during the main mission phase. In order to maximize utilisation of the APPU engine and minimize kerosene use, a target thrust share was iteratively determined for each of the sizing missions c1–c3 in table 2, with the aim of burning all available H_2 either by the end of the diversion (c1) or by the end of the main phase (c2 and c3). In the case of c2 and c3, this thrust share exceeds the thrust capability of the APPU engine for some part of the range. In this case, APPU thrust was limited to full throttle until the total thrust requirement reduced sufficiently, and afterwards thrust share was held constant until the end of the mission. Similarly, all "LH_2" phases (i.e. where the APPU engine is operating but not using H_2), assume that the APPU engine runs at full throttle throughout, thus maximizing thrust share in order to benefit from the lower $tsfc$ to the largest extent possible. During the sizing missions c4–c6, no LH_2 may be consumed at all, despite carrying a full LH_2 tank.
While the respective component failures assumed in the engine and fuel mass sizing process are expected to be too likely to neglect the implications for safety, they are still assumed to be rare exceptions to the operational routine. Thus, the impact of the different reliability scenarios on block fuel burn was evaluated for nominal operations, i.e. assuming that the APPU engine and H_2 fuel system work normally, while carrying the appropriate amount of spare kerosene to provide the necessary reserves determined in the sizing process.

3. Results

3.1 LH_2 tank and tailcone redesign

Based on a geometrical analysis, it was found that a capacity of 832kg usable H_2 is possible, which leads to an estimated tank mass of 956kg, including residual H_2 and associated fuel systems. The resulting gravimetric efficiency (η_{grav}) is 46.5%. This is treated as added mass compared to the reference aircraft. It may be possible to reduce the structure mass somewhat, by making the tank a structurally-integral part of the tailcone or by using a fibre composite structure, but due to the uncertainty in estimating the resulting benefits to structure mass, it was decided to use the more conservative estimate. The effect of reshaping the rear part of the fuselage tailcone was investigated using RANS CFD, and the resulting flow fields are shown in figure 5. It can be seen that the tailcone up-sweep leads shear lines to converge towards the upper part of the tailcone, which indicates the beginnings of vortex roll-up. While the phenomenon is very weak in the reference case, the modified tailcone exhibits this to a much higher degree, although analysis of the 3D flow field found no clear vortex formation, which is likely inhibited by the very thick boundary layer over this part of the fuselage. The modified tail was found to increase the overall drag coefficient by $4 \cdot 10^{-4}$, which corresponds to about 1% of total aircraft drag in cruise (H=10054.8m, M=0.78).

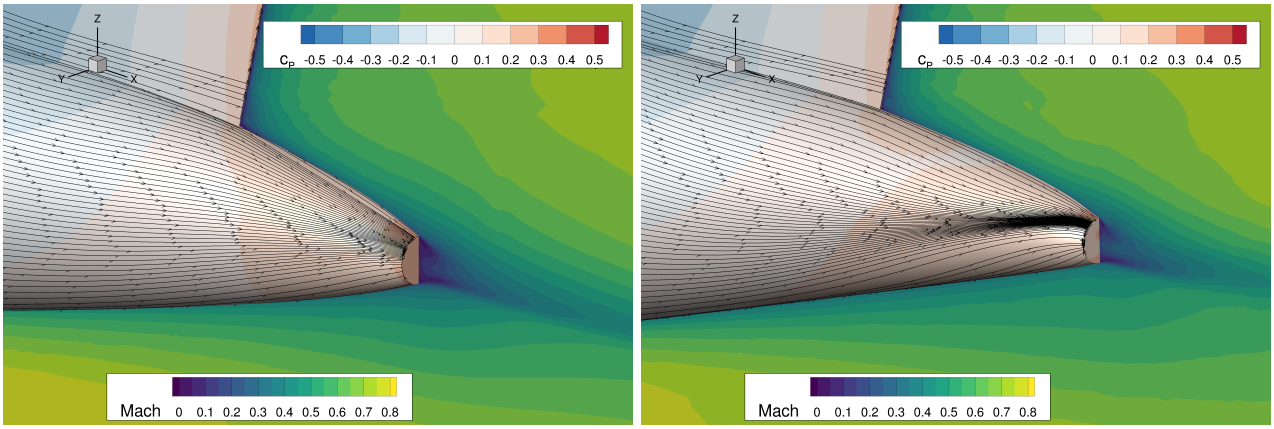

Figure 5 – RANS simulation results of flow around the reference tail (left) and the modified tail (right) at cruise conditions (M=0.78, α=1.5°), showing Mach number in the symmetry plane, pressure coefficient and shear lines on the surface.

3.2 BLI performance

In order to investigate the relationship between power applied by the BLI propulsor and its effect on the overall balance of forces, an actuator disk was implemented, using a body force model which adds axis-parallel momentum to the flow passing through the volume occupied by the BLI rotor, thus imposing a force on the fluid. This corresponds to a perfect lossless BLI rotor, since both swirl and the entropy increase from viscous and compressibility losses on the blades are not regarded. The simulations were conducted with 0, 2MW and 4MW actuator power, and showed a clear linear trend, which permits interpolation to arbitrary disk power. One observation was that ΔNVF_{prop} (see equation 3), i.e. the propulsive benefit produced by the actuator, is about 15% less than the force on the actuator disk itself. This is explained by the conical surface on which the actuator operates. Figure 6 shows the pressure field obtained with a preliminary radial load distribution and a total rotor power of 2MW, using a symmetric domain, and the difference in static pressure which the actuator creates. It is clearly visible that the actuator causes a reduction in static pressure in the upstream flow field which causes a force on the tailcone which acts in downstream direction, thus counteracts the upstream force created by the actuator. Conversely, the pressure downstream of the actuator is increased but cannot cancel this effect since it acts on a much smaller surface area. This means that an aircraft with rear-mounted open rotor of this type is to some extent "pulling on its own tail", which in turn uses up a certain amount of the power which it applies to the fluid.

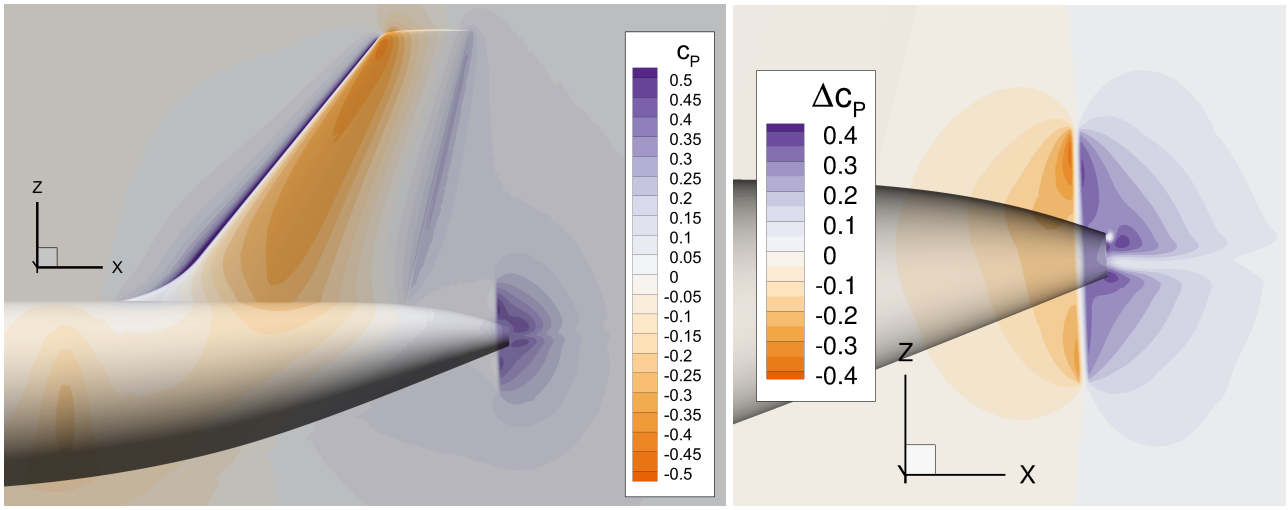

Figure 6 – Pressure coefficient on the surface and symmetry plane around the modified tailcone, using a preliminary radial load distribution, no exhaust mass-flow and 2MW actuator power. M=0.78, α=1.5°, H=10058.4m

The BLI propulsor provides a ΔNVF_{prop}=8.97kN with an actuator power of P_{act}=2MW. This is about 8% more than the force on an ideal free-stream propulsor of equal size, operating in undisturbed flow, with equal power. In addition to this beneficial effect, the slower-moving flow on the fuselage tailcone is also expected to reduce the efficiency penalty for an open rotor in transonic flow since the axial Mach number at the rotor tip location does not exceed 0.7, despite the aircraft cruising at M=0.78.

3.3 APPU engine tsfc

Following the methodology laid out in section 2.5, the effect of the engine core and propulsor were determined separately, using RANS simulations. For this purpose, the CFD geometry was adapted to include a submerged inlet and exhaust, and the engine core mass-flow imposed on both intake and exhaust, with the total temperature of the exhaust corresponding to the engine cycle model. This was used to calculate $\Delta NVF_{core,cr}$. The effect of the propulsor was derived from separate simulations using an actuator disk of varying power, from which the effect on overall forces as a function of actuator power can be interpolated. Since the actuator disk dos not produce any losses, a propulsor efficiency of η_{prop}=0.88 was assumed, which means that only 1760kW of the 2MW shaft power are applied to the actuator. A separate design study found a thermal efficiency of 44.5% achievable[17] for the APPU engine core, however this study assumed a reduced value of 43%, to account for any installation penalties, e.g. increased cooling bleed for the propulsor gearbox. This leads to an overall $tsfc'_{H_2}$=4.3$\frac{g}{s \cdot kN}$ at ToC, when operating on H_2 fuel. Table 3 shows the component values (see also equation 7), and table 4 shows the specific fuel consumption assumed in the fuel burn analysis, for the APPU engine as well as for the different underwing turbofan engines.

var	value	unit	comment
η_{core}	0.43	–	from engine cycle model
η_{prop}	0.88	–	
$P_{act,cr}$	1760	kW	2MW shaft power times η_{prop}
ΔNVF_{prop}	7.9	kN	from RANS analysis with actuator disk
$\Delta NVF_{core,cr}$	1.1	kN	from RANS analysis with intake and exhaust
$tsec$	514	$\frac{W}{N}$	see equation 7

Table 3 – efficiencies, net vehicle forces at ToC condition and the resulting effective $tsec$ values for the APPU engine

	$tsfc_{cruise}(\frac{g}{s\,kN})$ kerosene	H_2	m_{inst} (t)	ToC thrust (kN)
LEAP-1A33 (reference)	14.3		4.89	30.3
new TF (LEAP replacement)	13.1		5.22	30.4
new TF (minimum size)	13.0		5.03	26.3
APPU	12.0	4.30	1.74	9.0

Table 4 – Specific fuel consumption, installed mass and ToC thrust for the turbofan engine on the reference aircraft, the next-generation turbofan (sized as standalone replacement with reduced design thrust), and the APPU engine.

By comparison to the conventional turbofan engines on the reference aircraft, this finds a 16% improvement in fuel efficiency. The fairly large contribution of the engine core to the force balance can be explained by the fact that the intake ingests slow-moving air from the near-wall boundary layer, and exhausts into the region at the tailcone base, which has $c_P > 0.2$. This means that the "ram drag" component in the engine core force balance is quite low, since the ingested air is actually accelerated in the intake. Simultaneously, the hot exhaust gas is released at comparatively high static pressure at the base of the tailcone, thus reaches higher downstream Mach numbers than it would with a conventional turboprop arrangement. In short: While the engine core efficiency is negatively affected by the low intake total pressure and the exhaust counter-pressure, its propulsive force balance benefits

considerably from the BLI effect. It is believed that the adverse effect on core efficiency is greater than the benefit derived this way, but that an intake able to deliver air at close to free-stream total pressure would be difficult to design, integrate, and likely to cause considerable distortion for the BLI propulsor.

3.4 Main Engine Upgrade

As shown in figure 3, the next-generation turbofan engine has a roughly 8.8% lower $tsfc$ than the current engines, at equal thrust requirement. In order to demonstrate the separate effects of the APPU conversion and a main engine upgrade, a "stack-up" study was conducted with incremental changes applied to the baseline reference. The resulting design scenarios are explained in table 5.

label	Main engines	APPU mod.	comment
`A321neo`	LEAP-1A	no	reference
`LEAP+APPU`	LEAP-1A	yes	"naïve" addition of APPU
`A321v3`	new TF	no	conventional upgrade scenario
`v3+APPU`	new TF	yes	addition of APPU to `A321v3`
`resized`	new TF, resized	yes	TF thrust adapted to APPU

Table 5 – Overview of the different designs generated for the incremental study. "APPU mod." refers to the addition of the APPU engine and LH_2 tank, as well as reshaping the tailcone and reconfiguring the empennage.

In each scenario, it was assumed that the APPU engine operates at constant thrust share, determined such that all available LH_2 is used up during the mission and diversion, but is not using kerosene at all. This resulted in a nominal thrust share just below 15%. The resulting kerosene use of the different designs is shown in figure 7. The upgrade of the underwing engines yields a 9% reduction in kerosene

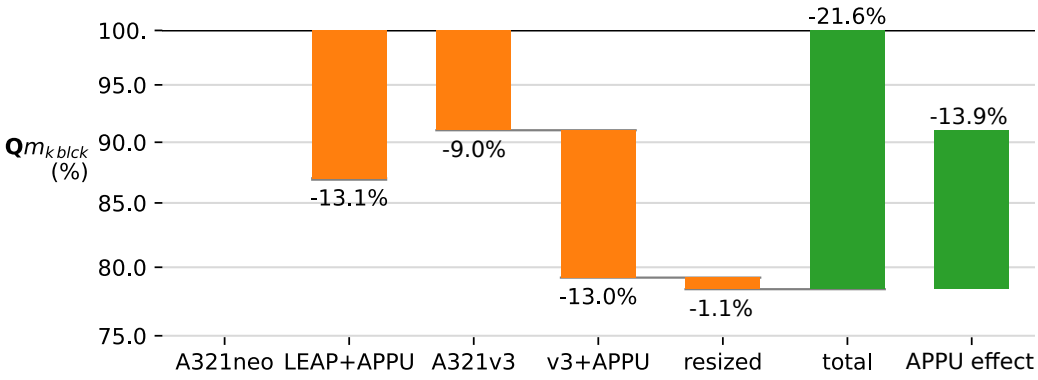

Figure 7 – Change of block kerosene use, relative to the A321neo baseline for the various engine design scenarios. The two rightmost columns show summarize the total benefit of all considered changes over the baseline, and the part of these benefits which is enabled by adding the APPU unit.

burn, thus marginally exceeding the reduction in $tsfc$, since the reduced fuel mass compensates for the increased engine mass. On its own, adding an APPU unit to the baseline configuration reduces kerosene burn (and with it, CO_2 emissions) by about 13%, 45% more than a conventional engine upgrade. This benefit of adding the APPU unit is almost independent of the main engines are also upgraded or not, meaning that the addition of an APPU unit does not need to be regarded as an *alternative* to a main engine upgrade but rather as an *additional* measure which provides a benefit independently of the main engines. However, if the main engines are also upgraded, the added thrust from the APPU engine permits reducing the thrust requirement on the new turbofan engines, which in turn reduces both main engine mass and $tsfc$ further, yielding an additional 1.1% benefit of combining both upgrades. Overall the analysis finds that a total kerosene burn reduction of 21.6% is possible for the reference mission, compared to the reference aircraft. This is the same benefit as about 2.5 consecutive engine upgrades.

3.5 Reliability and Operational Considerations

Figure 8 summarizes te outcome of the fuel burn analysis for all configurations resulting from the different reliability scenarios, in terms of block energy use and block emissions metric, relative to the reference A321neo aircraft. The comparison also includes the *A321v3* and the other configurations shown in figure 7.

The comparison in figure 8 confirms that block energy is largely dictated by the choice of the main underwing engines while the addition of an APPU engine provides a benefit to block emissions which is considerably larger than the benefit of an engine upgrade, and this benefit is largely independent of the main engines it is paired with. The main effect of the APPU conversion is the ability to substitute kerosene with hydrogen, thus reducing the climate impact for a given block fuel energy. This becomes visible in comparing the `LEAP+APPU` to the A321neo reference, and the `v3+APPU` configuration to the `A321v3`: In both cases the relative kerosene burn reduction achieved by including the APPU engine is almost exactly equal (see also figure 7). The minor increase in block energy in the latter case, is due to the fact that since the efficiency improvement of the APPU engine over the main engines is too low to compensate for the mass added by the APPU installation. Resizing the main engines (configuration `c1`) improves their efficiency and reduces weight, which brings back fuel energy use to the same level as without the APPU engine.

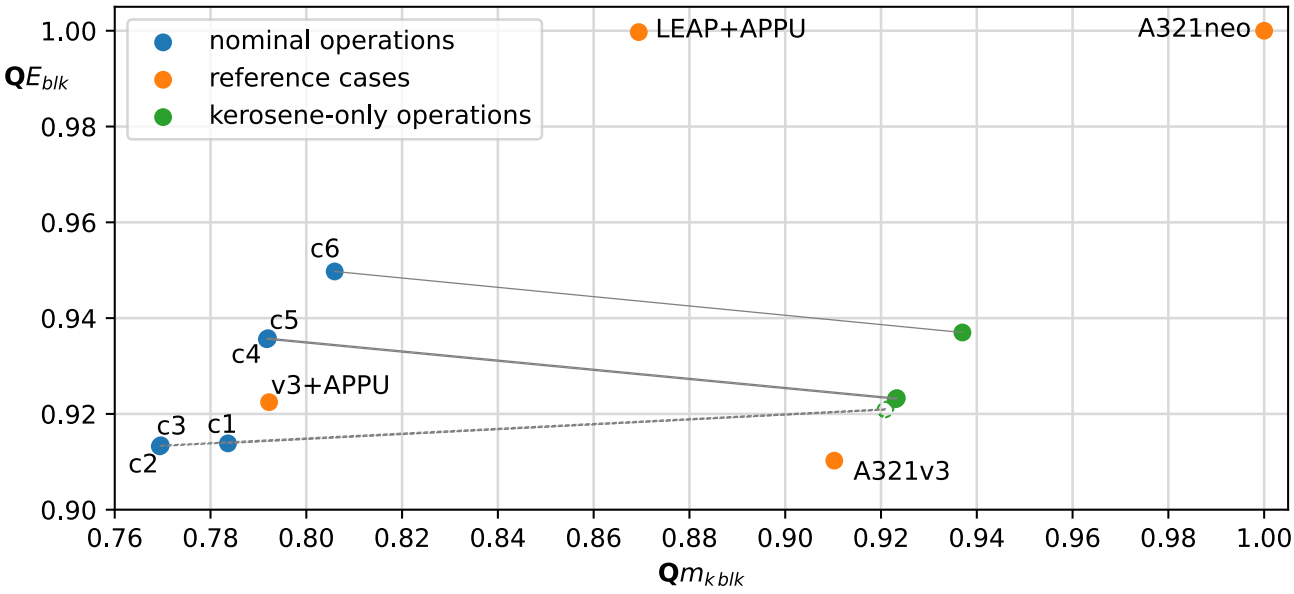

Figure 8 – Relative block kerosene burn and fuel energy use for the reference mission. Reference cases are the configurations shown in figure 7. Lines indicate data for the same configuration during nominal and kerosene-only operations. Dashed symbols indicate configurations which don't meet the OEI thrust criterion for the design range with full payload.

Another observation is that the lowest block kerosene burn, and thus CO_2 emissions, is achieved by configurations sized for reduced reliability. Between configurations `c2` through `c6`, block fuel increases in line with more pessimistic sizing scenarios, but all configurations except `c1` do not rely on H_2 for the diversion and can thus use all available H_2 during the main segment of the flight. As a consequence, the configurations `c2` and `c3` achieve the lowest kerosene use since they can have sufficient LH_2 available to keep the APPU engine at maximum throttle for the first half of the flight, at which point the total thrust requirement has reduced sufficiently for the APPU to provide about 17% of total thrust, and maintain a constant thrust share after this. This operational strategy reduces kerosene burn by about 2% compared to the `c1` configuration which needs to keep LH_2 reserves for the diversion. In total, `c2` and `c3` have 23% lower CO_2 emissionas than the A321neo, and 15.5% less than the re-engined reference `A321v3`, despite a maximum achievable thrust share of only 14.5% at ToC.

This means that choosing to size the main engines and kerosene fuel reserves with the assumption of reduced reliability of the APPU engine and fuel systems in critical situations does not only permit

reducing development time and cost and safety risks, but also minimizes CO_2 emissions.
Another operational scenario of note is kerosene-only operations. This scenario assumes that there is no hydrogen available upon departure, and the refuelling amount of kerosene is adjusted accordingly before departure. In this scenario, the LH_2 tank is assumed to carry 10% of the usable amount of hydrogen, in order to prevent thermal cycling during the flight, but the APPU engine is operating on kerosene, and at 100% throttle. For the certification scenarios `c1` – `c3`, the additional kerosene increases the required take-off mass beyond the amount needed for the design mission, which means that they would not be able to meet the required OEI thrust and thus not be permitted to fly the reference mission. These configurations would thus be limited somewhat in either payload or range in kerosene-only operations, and the data points have been marked accordingly in figure 7. Independent of this, the results show that all certification variants whose design mission uses no H_2 (`c4` – `c6`) have reduced block energy consumption when operating on kerosene. This is due to the fact that their design missions require them to carry sufficient kerosene for the entire mission at all times, and this acts as dead weight when it is not used. In the kerosene-only scenario, they are able to burn the heavy kerosene instead of lighter hydrogen, reducing aircraft mass compared to the nominal mission. This does however not make them more efficient than the `c1` - `c3` configurations, since they still need to use heavier and less efficient main engines. Overall, configurations `c1` - `c5` in kerosene-only operations exceed the fuel burn of the `A321v3` by about 1%, which is rather modest compared to the benefit during nominal operations.

3.6 Conclusions

The results show that replacing the APU unit on a A321neo aircraft (and by extension on other similarly configurations) with a hydrogen-driven APPU unit has the potential to reduce CO_2 emissions by a fraction exceeding its nominal ToC thrust share. Take-off mass of the modified aircraft is reduced since the lower fuel mass compensates for the added structure and systems mass.
In combination with a main engine upgrade to 2035 technology level, the total reduction of CO_2 emissions is predicted to be 23%, compared to 9% for a main engine upgrade alone. This means that addition of the H_2-driven APPU yields a 15.5% CO_2 reduction, with 14.6% ToC thrust share. This can be decomposed into multiple effects. Adding the APPU engine without changing the main engines yields about 13% reduction in kerosene burn, by displacing some of the kerosene with hydrogen as energy source. The effect is smaller than the thrust share produced from H_2, due to the added mass and drag from APPU engine installation, and is independent of the choice of main engines. Resizing the main engines with a suitably reduced thrust requirement increases their efficiency and reduces mass, resulting in about 1% further reduction of both CO_2 emissions and block energy use. An additional 2% reduction in CO_2 emissions (with minor reduction in block fuel energy) can be achieved if the main engine size and kerosene fuel reserves are adapted such that a failure of the APPU engine and LH_2 fuel system may not lead to a safety-critical situation, and does not need to be relied on for the diversion. This permits the APPU engine to consume all usable H_2 fuel onboard before the start of the diversion and increase the effective thrust share.
This operational and sizing strategy permits the APPU engine and H_2 fuel systems to have reduced reliability compared to conventional engines and fuel systems, without impacting aircraft safety. In addition to the immediate reduction of the climate impact, it is expected that this can speed up both development and market adaptation. The operation, maintenance and repair of hydrogen-driven aero engines and BLI propulsion, in turn, is required to mature the technology to the point where it can play a much greater role in achieving climate-neutral aviation.

3.6.1 Recommendations

The outcomes of this study are sensitive to the estimate of the APPU engine's effective $tsfc$' and achievable thrust, therefore more accurate modelling of the BLI propulsor performance could permit a better estimate of the achievable efficiency both in cruise and in other conditions. This would simultaneously permit an update of the results presented here, and provide the input needed for a fuel burn analysis which includes the climb and descent phases, and thus enable higher-fidelity mission analysis throughout the entire payload/range envelope. This is of particular interest for shorter routes or with lower payload, where the lower overall thrust requirement would permit the APPU engine to

provide a larger share of overall propulsive energy without using kerosene. Analysing the impact of the APPU engine on missions of varying range and payload permits further studies into operational strategies and sizing criteria.
Another point of interest is a potential trade-off of thrust capability versus efficiency, since higher thrust share has been shown to reduce CO_2 emissions but is expected to degrade the efficiency with which the LH_2 is used. Such an investigation would require the ability to obtain thrust and efficiency estimates for APPU engines and propulsors of varying size and power.
Another area of interest is the impact of the APPU engine on LTO emissions. While it is not clear if the APPU engine could achieve break-away thrust, it seems plausible that it could cover most taxi operations without requiring the main engines which are operating at very low efficiency while taxiing, and could therefore provide considerable benefits, both by virtue of operating more efficiently during taxi and being able to entirely avoid local emissions from carbohydrate fuels. It is less clear how large of a benefit the APU engine can provide while providing onboard power, compared to dedicated APU, and what the noise levels during gate operations and in taxi are, compared to a conventional configuration.
While having a lesser impact on design decisions, a refinement of component mass estimates is expected to improve confidence in the current results. Since the H_2 fuel system forms a major part of the total LH_2 tank mass, a more reliable estimate would be desirable, although the path to obtain it is not currently clear. Some work to establish and/or refine the mass and drag estimate of the reconfigured empennage is currently underway, as is an investigation into the structural configuration of an integral LH_2 tank, with the aim of determining the feasibility of such a configuration and its impact on mass.

Copyright Statement

References

[1] Smith L H. Wake ingestion propulsion benefit. *Journal of Propulsion and Power*, Vol. 9, No. 1, pp 7482, 1993 https://doi.org/10.2514/3.11487

[2] Drela M. Development of the D8 Transport Configuration. *29th AIAA Applied Aerodynamics Conference*, Honululu, Hawaii, AIAA 20113970, 2011 https://doi.org/10.2514/6.2011-3970

[3] Della Corte B, van Sluis M, Gangoli Rao A and Veldhuis L L. *Aerodynamic performance of an aircraft with aft-fuselage boundary layer ingestion propulsion*. AIAA Aviation Forum, 2021. https://doi.org/10.2514/6.2021-2467

[4] Seitz A, Habermann A L, Peter F, Troeltsch F, Castillo Pardo A, Della Corte B, van Sluis M, Goraj Z, Kowalski M, Zhao X, Grönstedt T, Bijewitz J and Wortmann G. Proof of Concept Study for Fuselage Boundary Layer Ingesting Propulsion. *Aerospace*, Vol. 8, No. 1, p 16, 2021 https://doi.org/10.3390/aerospace8010016

[5] Heidebrecht A, Burger K, Hoogreef M, Vos R, Isikveren A T and Gangoli Rao A. Development of a hydrogen-powered fuselage-mounted BLI propulsor add-on for passenger aircraft. *33rd Congress of the International Council of the Aeronautical Sciences*, ICAS2022-0622, 2022. http://www.icas.org/ICAS_ARCHIVE/ICAS2022/data/papers/ICAS2022_0622_paper.pdf

[6] Heidebrecht A, Hoogreef M, Vos R, Isikveren A T and Gangoli Rao A. Preliminary Design of an Auxiliary Hydrogen-powered Fuselage-mounted BLI Propulsor for Passenger Aircraft. in preparation, 2024

[7] Elmendorp R, Vos R, La Rocca G. *A conceptual design and analysis method for conventional and unconventional airplanes*. 29th Congress of the International Council of the Aeronautical Sciences (St. Petersburg, Sept. 2014), ICAS.

[8] Airbus. *A321 Aircraft Characteristics, Airport and Maintenance Planning*, Apr. 2020.

[9] EASA. *Type-Certificate Data Sheet for Engine LEAP-1A & LEAP-1C series engines*, May 2018.

[10] Onorato G, Proesmans P, and Hoogreef M F M. Assessment of Hydrogen Transport Aircraft. *CEAS Aeronautical Journal*, Vol. 13, No. 4, pp 813-845, 2022 https://doi.org/10.3390/aerospace8010016

[11] Stautner W., Ansell P., Haran K. Mariappan D. D. and Minas C.. Liquid hydrogen tank design for medium and long range all-electric-airplanes, *CEC / ICMC 21 virtual conference*, IOP Conference Series: Materials Science and Engineering, no. C3OR1A05, July 2021

[12] Fesmire J E, Augustynowicz S D and Scholtens B E. Robust Multilayer Insulation For Cryogenic Systems, *AIP Conference Proceedings*, Vol. 985, No. 1, pp 1359-1366, 2008 https://doi.org/10.1063/1.2908494

[13] Oom Ortiz de Montellano T. Structural Analysis of a New Integral Tank Concept for Hydrogen Storage On-board Commercial Aircraft, *MSc thesis, Delft University of Technology*, April 2024

[14] Proesmans P-J and Vos R. Airplane Design Optimization for Minimal Global Warming Impact. *Journal of Aircraft*, Vol. 59, No. 5, pp 1363-1381, 2022 https://doi.org/10.2514/1.C036529

[15] *ICAO Aircraft Engine Emissions Databank*. queried May 2023, https://www.easa.europa.eu/en/domains/environment/icao-aircraft-engine-emissions-databank

[16] Kurzke J and Halliwell I. *Propulsion and Power: An Exploration of Gas Turbine Performance Modeling*, 1st edition, Springer Cham, Switzerland, May 2018, ISBN 978-3-030-09370-9

[17] van Schie M. Steam injection and recovery in the APPU, *MSc thesis, Delft University of Technology*, planned publication: June 2024

[18] MIDAP Study Group. AGARDograph No. 237: Guide to In-Flight Thrust Measurements of Turbojets and Fan Engines, AGARD-AG-237, 1976

[19] Barış A. Inlet Design for a Propulsive Fuselage Concept: Exploring and evaluating geometrical inlet features based on a numerical approach, *MSc thesis, Delft University of Technology*, April 2024

[20] Mourouzidis C et al.. Abating CO2 and non-CO2 emissions with hydrogen propulsion, *The Aeronautical Journal*, pp. 1-18, 2024 https://doi.org/10.1017/aer.2024.20

[21] van Schie M. Steam injection and recovery in the APPU, *MSc thesis, Delft University of Technology*, July 2024

[22] EASA. *Certification Specifications and Acceptable Means of Compliance for Large Aeroplanes (CS-25)*, Amendment 27, November 2021.

[23] EASA. *Certification Specifications for Auxiliary Power Units (CS-APU)*, October 2003.